Inorg. Chem. **2009**, *48*, 1482−1489

Self-Assembly of Ambivalent Organic/Inorganic Building Blocks Containing Re_6 Metal Atom Cluster: Formation of a Luminescent Honeycomb, Hollow, Tubular Metal-Organic Framework

Michael A. Shestopalov,[†,‡] Stéphane Cordier,[*,†] Olivier Hernandez,[†] Yann Molard,[†] Christiane Perrin,[†] André Perrin,[†] Vladimir E. Fedorov,[‡] and Yuri V. Mironov[*,‡]

Sciences Chimiques de Rennes, UMR 6226 CNRS - Université de Rennes 1, Avenue du Général Leclerc, 35042 Rennes Cedex, France, and Nikolaev Institute of Inorganic Chemistry, Siberian Branch of Russian Academy of Sciences, 3 Acad. Lavrentiev Prosp., 630090 Novosibirsk, Russia

Received September 24, 2008

Reactions in a sealed glass tube between melted pyrazine (pyz) and a $Cs_3Re_6Q^i_7Br^iBr^a_6 \cdot H_2O$ inorganic rhenium cluster compound (Q = S, Se; "i" for inner and "a" for apical positions) containing $[Re_6Q^i_7Br^iBr^a_6]^{3-}$ units led to the substitution of three apical bromine ligands by three pyrazine groups with the formation of 3 CsBr as a byproduct. The resulting *fac*-$Re_6Q^i_7Br^i(pyz)^a_3Br^a_3$ building unit, based on a Re_6 metal atom cluster, is neutral and noncentrosymmetric and exhibits an ambivalent organic/inorganic nature owing to the opposite disposition of the three apical pyrazine groups versus the three apical bromine atoms. These compounds were characterized by single-crystal and powder X-ray diffraction, elemental and thermal analyses, and luminescence measurements. The crystal structure of *fac*-$Re_6Q^i_7Br^i(pyz)^a_3Br^a_3 \cdot xH_2O$ (Q = S (**1**) and Se (**2**)) displays an original, neutral metal-organic framework based on the self-assembling of *fac*-$Re_6Q^i_7Br^i(pyz)^a_3Br^a_3$ hybrid building units. The latter are held together by supramolecular interactions: $\pi-\pi$, hydrogen bonds (C−H···N, C−H···Br^a, and C−H···Br^i), and van der Waals contacts. It gives rise to a honeycomb porous structure of parallel hollow open-ended channels wherein the water molecules are located. Their removal does not lead to the collapsing of the structural edifice. The channel walls are constituted by hydrogen atoms from pyrazine as well as apical bromine from the cluster unit. To our knowledge, the structures of **1** and **2** constitute with that of PTMTC (perchlorotriphenylmethyl functionalized by carboxylic group radicals) one of the rare examples of stable open frameworks stabilized by supramolecular interactions between neutral molecules. Moreover, **1** is the first example of luminescent Re_6 compound built up from a noncentrosymmetric $Re_6S^i_7Br^i$ cluster core.

Introduction

Octahedral rhenium cluster complexes with the general formula $[Re_6Q^i_{8-y}X^i_yL^a_6]^{(4-y)-}$ (Q = S, Se, Te; X = Cl, Br, I; L = organic ligands; "i" for inner and "a" for apical positions[1]) have been subjected to intense investigations for many years.[2] Research in this area is actually motivated by the complexes' nanosized shape and their structural, redox, and photoluminescence properties, which make them relevant building blocks for the elaboration of supramolecular assemblies and nanomaterials.[3] In this work, the synthesis in mild conditions and the characterizations of an original metal organic framework (MOF) with a porous architecture based on metal atom clusters are presented. Inorganic compounds based on $[Re_6Q^i_{8-y}X^i_yX^a_6]^{(4-y)-}$ units containing octahedral rhenium clusters have been reported in the literature for a long time.[2] They are synthesized via high-temperature solid-state techniques in silica containers. The Holm and Zheng groups in the 1990s started the coordination chemistry of octahedral cluster complexes using inorganic precursors

* To whom correspondence should be addressed. Phone: +33 2 23 23 65 36(S.C.). Fax: +33 2 23 23 67 99 (S.C.), +7-383-3309489 (Y.V.M.). E-mail: stephane.cordier@univ-rennes1.fr (S.C.), yuri@che.nsk.su (Y.V.M.).
† Université de Rennes 1, UMR 6226 CNRS.
‡ Siberian Branch of Russian Academy of Sciences.

(1) Schäfer, H.; von Schnering, H.-G. *Angew. Chem.* **1964**, *20*, 833.

(2) Selected references: (a) Bronger, W.; Spangenberg, M. *Acta Crystallogr.* **1978**, *A34*, 168. (b) Perrin, A.; Sergent, M. *Eur. New J. Chem.* **1988**, *12*, 337. (c) Fedorov, V.; Mishenko, A.; Kolesov, B. *Bull. Acad. Sci. USSR Div. Chem. Sci.* **1984**, *33*, 1976. (d) Long, J. R.; MacCarty, L. S.; Holm, R. H. *J. Am. Chem. Soc.* **1996**, *118*, 4603, and references therein.

10.1021/ic8018277 CCC: $40.75
Published on Web 01/16/2009

synthesized at high temperatures. Indeed, after their dissolution in aqueous solutions, the precipitation of $[Re_6Q^i_8X^a_6]^{n-}$ units with tetrabutylammonium $((n\text{-}C_4H_9)_4N)^+$ organic cations affords $((n\text{-}C_4H_9)_4N)_n[Re_6Q^i_8X^a_6]$ ($n = 4$ for S, $n = 3$ for Se) precursors, from which a wide variety of hybrid $[Re_6Q^i_8L^a_6]^{2+}$ units based on a $Re_6Q^i_8{}^{2+}$ inorganic cluster core and functional organic moieties utilized as apical ligands can be prepared (L = N- and P-donor ligands).[3−6] For instance, hexasubstituted $[Re_6Q^i_8L^a_6]^{2+}$ functional units were prepared from $[Re_6Q^i_8I^a_6]^{3-}$ units (Q = S, Se) after the prior removal of iodine apical ligands from the cluster core by reaction with silver salt in order to facilitate the apical ligand substitution. On the other hand, partially substituted $[Re_6Q^i_8(PEt_3)^a_{6-x}I^a_x]^{(2-x)+}$ units were synthesized by direct reaction of $[Re_6Q^i_8I^a_6]^{3-}$ units with PEt_3, leading to a set of $[Re_6Q^i_8(PEt_3)^a_{6-x})I^a_x]^{(2-x)+}$ anionic units with different x values and possible isomeric units. The Re−P bonds being very strong, functional $[Re_6Q^i_8(PEt_3)^a_{6-x})L^a_x]^{2+}$ units were obtained after prior reactions of $[Re_6Q^i_8(PEt_3)^a_{6-x}I^a_x]^{(2-x)+}$ with silver salt in order to remove the apical iodine atoms. Beyond various types of functional Re_6 supramolecular units, this technique afforded original MOFs based on hydrogen-bonding networks by grafting, for instance, isonicotinamide on the cluster.[6] It turns out that the lower reactivity of the $Re_6S^i_8$ cluster cores compared to that of $Re_6Se^i_8$ leads to a smaller set of supramolecular assemblies with sulfur than with selenium. In order to functionalize $[Re_6Q^i_{8-y}X^i_yX^a_6]^{(4-y)-}$ units, a simple original approach that works for both sulfide and selenide homologs has been developed recently. It consists of the direct reaction of the $Cs_{4-y}[Re_6Q^i_{8-y}X^i_yX^a_6]$ salt with melting N-, P-, As-, and Sb- donor ligands.[7] This method is an effective way for obtaining clusters with organic ligands using oxidized and non-oxidized anion complexes $[Re_6Q^i_{8-y}X^i_yX^a_6]^{(4-y)-}$ (Q = S, Se; X = Cl, Br, I). The limiting factor of the technique is the thermal stability of organic ligands that can decompose before the exchange occurs. Among organic ligands stable at mild temperatures, bidendate linkers such as, for instance, bipyridine or pyrazine constitute relevant candidates to build coordination polymers with low dimensionalities or supramolecular frameworks. In the present work, the interactions of $Cs_3Re_6Q_7Br_7\cdot H_2O$ (Q = S, Se) complexes[8] with melted pyrazine (pyz) have been investigated. *fac*-$Re_6Q^i_7Br^i(pyz)^a_3Br^a_3\cdot xH_2O$ compounds (Q = S (**1**), Se (**2**)) constitute the first cluster-based hybrid framework whose structural cohesion results only from supramolecular interactions between units ($\pi-\pi$ interactions, hydrogen bonds, Q···Br van der Waals contacts). Complexes **1** and **2** were characterized by powder and single-crystal X-ray diffraction, elemental and thermal analyses, and luminescence measurements. The solvent water molecules can easily be removed by thermal treatment without breaking the structure. The structural findings will be discussed and compared with relevant organic and metal-organic frameworks based on a similar topology.

Experimental Section

General Informations. Elemental analyses (C, H, N, S) were performed at the Centre Régional de Mesures Physiques de l'Ouest (CRMPO), Rennes, France, using a Microanalyzer Flash machine (EA1112 CHNS/O Thermo Electron). Energy dispersive spectroscopy (EDS) was performed on a JEOL 6400 scanning electron microscope equipped with a XEDS Oxford field spectrometer. Infrared spectra were recorded on KBr pellets using a Bruker Equinox SS spectrophotometer. The thermal properties were studied on Setaram Labsys TG, DTA/DSC in the temperature range 25−350 °C with a rate of 5°/min in a N_2 flow.

Single-crystal X-ray diffraction data were collected using graphite monochromatized Mo Kα radiation ($\lambda = 0.71073$ Å) at 293 K on a Bruker Nonius X8Apex diffractometer equipped with a CCD area detector. The φ-scan technique was employed to measure intensities. Absorption corrections were applied using the SADABS program.[9] The powder X-ray diffraction patterns were recorded up to 120° 2θ with very good counting statistics on a BRUKER AXS D8 Advance diffractometer ($\theta-\theta$ Bragg−Brentano geometry) using monochromatic Cu $K_{\alpha 1}$ radiation and a linear position sensitive detector (Braun L-PSD).

Luminescence spectra were recorded on powdered samples at room temperature using a Cary Varian (Eclipse) spectrophotometer. The excitation wavelength was 450 nm.

Synthesis of *fac*-$Re_6Q^i_7Br^i(pyz)^a_3Br^a_3\cdot xH_2O$ (Q = S (1) and Se (2)). The $Cs_3[Re_6Q_7Br_7]\cdot H_2O$ (Q = S, Se) inorganic precursors were synthesized in a sealed silica ampule by high-temperature reactions using methods described in the literature.[8] Pyrazine (≥99%) was purchased from Aldrich and used as received. Several experiments were carried out using different reaction temperatures and $Cs_3[Re_6Q_7Br_7]\cdot H_2O$/pyrazine ratios heated for typical reaction times of 2 days in order to optimize the experimental procedure. In the range 110−140 °C, $Cs_3[Re_6Q_7Br_7]\cdot H_2O$ did not fully react with pyrazine. From 140 to 170 °C, the reaction was total with almost quantitative yield for a $Cs_3[Re_6Q_7Br_7]\cdot H_2O$/pyrazine ratio close to 0.2:5. For temperatures higher than 170 °C, the pyrazine group started to decompose. After the optimization procedure, the molecular octahedral rhenium cluster complexes *fac*-$Re_6S^i_7Br^i(pyz)^a_3Br^a_3\cdot xH_2O$ (**1**) and *fac*-$Re_6Se^i_7Br^i(pyz)^a_3Br^a_3\cdot xH_2O$ (**2**) were synthesized at 140 °C for 2 days in a sealed glass tube by reactions of the corresponding ionic chalcobromide complexes $Cs_3[Re_6S_7Br_7]\cdot H_2O$ (500 mg = 0.22 mmol) and $Cs_3[Re_6Se_7Br_7]\cdot H_2O$ (500 mg = 0.19 mmol)[8] with pyrazine (400 mg = 5 mmol). Single crystals

(3) (a) Selby, H. D.; Roland, B. K.; Zheng, Z. *Acc. Chem. Res.* **2003**, *36*, 933. (b) Roland, B. K.; Flora, W. H.; Carducci, M. D.; Armstrong, N. R.; Zheng, Z. *J. Cluster Sci.* **2003**, *14*, 449.

(4) (a) Yaghi, O. M.; Scott, M. J.; Holm, R. H. *Inorg. Chem.* **1992**, *31*, 4782. (b) Zheng, Z.; Long, J. R.; Holm, R. H. *J. Am. Chem. Soc.* **1997**, *119*, 2163–2171. (c) Willer, M. W.; Long, J. R.; McLauchlan, C. C.; Holm, R. H. *Inorg. Chem.* **1998**, *37*, 328.

(5) Gabriel, J.-C. P.; Boubekeur, K.; Uriel, S.; Batail, P. *Chem. Rev.* **2001**, *101*, 2037.

(6) Zheng, Z.; Long, J. R.; Holm, R. H. *Inorg. Chem.* **2003**, *42*, 1656.

(7) (a) Mironov, Y. V.; Shestopalov, M. A.; Brylev, K. A.; Yarovoi, S. S.; Romanenko, G. V.; Fedorov, V. E.; Spies, H.; Pietzsch, H.-J.; Stephan, H.; Geipel, G.; Bernhard, G.; Kraus, W. *Eur. J. Inorg. Chem.* **2005**, 657. (b) Mironov, Y. V.; Brylev, K. A.; Shestopalov, M. A.; Yarovoi, S. S.; Fedorov, V. E.; Spies, H.; Pietzsch, H.-J.; Stephan, H.; Geipel, G.; Bernhard, G.; Kraus, W. *Inorg. Chim. Acta* **2006**, *359*, 1129. (c) Shestopalov, M. A.; Mironov, Y. V.; Brylev, K. A.; Kozlova, S. G.; Fedorov, V. E.; Spies, H.; Pietzsch, H.-J. H.; Stephan, H.; Geipel, G.; Bernhard, G. *J. Am. Chem. Soc.* **2007**, *129*, 3714. (d) Shestopalov, M. A.; Mironov, Y. V.; Brylev, K. A.; FedorovV. E. *Russ. Chem. Bull.* **2008**,in press.

(8) Yarovoi, S. S.; Solodovnikov, S. F.; Mironov, Y. V.; Fedorov, V. E. *Mater. Res. Bull.* **1999**, *34*, 1345.

(9) *SADABS*, version 2.11; Bruker Advanced X-ray Solutions: Madison, WI, 2004.

were obtained once the reaction mixture was cooled down to room temperature at a rate of 10 °C/h. Complexes **1** and **2** are stable in the air and do not dissolve in water and organic solvents. Then, the excess of pyrazine was washed with ether, and the CsBr formed during the reaction was washed with water. Yield: 406 mg (97.6%) for **1** and 403 mg (94.5%) for **2**. Anal. calcd for $C_{12}H_{15}Br_4N_6O_{1.5}Re_6S_7$ (**1**): C, 7.43; H, 0.72; N, 4.38; S, 11.64. Found: C, 7.47; H, 0.78; N, 4.36; S, 11.64. Anal. calcd for $C_{12}H_{15}Br_4N_6O_{1.5}Re_6Se_7$ (**2**): C, 6.38; H, 0.67; N, 3.72. Found: C, 6.40; H, 0.66; N, 3.68. EDS shows the following Re/Q/Br ratios: 6:7:3.8 for **1** and 6:7.1:4.2 for **2**. IR spectra (400−4000 cm^{-1}) of compounds **1** and **2** display all peaks expected for pyrazine. In the spectrum of compound **1**, the band at 424 cm^{-1} may be assigned to Re-(μ_3-S) vibrations.

Thermogravimetric Analyses. The thermogravimetric analyses performed on the powder samples of **1** and **2** revealed a mass-loss step that has been attributed to water removal. TGA curves are given in the Supporting Information. The mass loss is completed around 110 °C for **1** and 90 °C for **2** and has been calculated to be 1.36% for **1** and 1.15% for **2**. It corresponds to 1.5 molecules of water per formula in both cases. After dehydration, the thermogravimetric curves of **1** and **2** remain parallel, with an inflection around 200 °C that can be attributed to the decoordination and evaporation of pyrazine. From these different analyses, the composition of powder was deduced to be $Re_6Q^i_7Br^i(pyz)^a_3Br^a_3 \cdot 1.5H_2O$ for **1** and **2**.

Powder X-Ray Diffraction Studies. The dehydration and rehydration processes were studied ex situ using X-ray powder diffraction. The samples were powders of **1** and **2** used for the thermogravimetric analyses. For the sake of comparison, sample **1** was soaked in water for 24 h at 70 °C in order to reach full hydration. Afterward, the same sample was dried for 24 h in the air at 110 °C to remove the water. On the other hand, sample **2** was first dried and then soaked using the same conditions as for **1**. A powder X-ray diffraction pattern was recorded promptly after each step. The experimental patterns of **1** and **2** were in very good agreement with the simulated patterns calculated from the single-crystal X-ray diffraction structural models. A whole-powder-pattern profile fitting procedure without structural constraints (Le Bail refinement, Thompson-Cox-Hastings profile function[10]) was performed through JANA2000[11] in order to refine the unit cell as well as the profile parameters. Due to the rather high unit-cell volume (~4000 $Å^3$), reflections appear for both compounds at a low angle (~7° 2θ). Despite the use of primary Soller slits, the profile of the latter lines is strongly affected by axial divergence. This usual aberration in powder diffractometry was partly corrected during the Le Bail refinements by the means of Finger's model, leading to satisfactory profile agreement factors. The six X-ray diffraction patterns collected could be fully indexed within the same unit cells and space group as those found using single-crystal diffraction. Unit-cell parameters are summarized in Table 1, and X-ray powder patterns of **2** are shown in the Supporting Information. Throughout the hydration and dehydration processes, the fwhm values do not increase as a whole for a given compound, indicating that no peculiar microstructural effect occurs during the transformation. For **2**, after rehydration, one can just notice the emergence in the background of a small bump around $2\theta \sim 10°$. The *c* refined unit-cell parameters obtained by powder X-ray diffraction for as-prepared **1** and **2** are higher within the s.u.'s than those obtained by single-crystal X-ray diffraction. On the other hand, for **1**, the unit-cell volume refined from powder X-ray diffraction data is lower than the one obtained by single-crystal X-ray diffraction (−37 $Å^3$), while for **2**, the opposite is observed (+14 $Å^3$). Two explanations can be proposed: single crystals have a slightly different content of water than the powder, which can be easily understood, or the unit-cell parameters from single-crystal data are not exactly comparable to the accurate values refined against the powder data. The most interesting point is that, after dehydration of **1** and **2**, the structural edifices do not collapse, as revealed by the shape of the powder patterns. The refined unit-cell parameters are smaller after dehydration, in agreement with the removal of water.

Table 1. Evolution of the Unit-Cell Parameters from Powder X-Ray Diffraction for **1** and **2** vs Hydration/Dehydration

	as prepared ($1.5H_2O$)	after hydration	after dehydration
1	a = 15.0150(4) Å c = 19.4254(6) Å V = 3792.7(2) $Å^3$	a = 15.0214(4)Å c = 19.4597(6) Å V = 3802.7 (2) $Å^3$	a = 15.0148(4) Å c = 19.4589(7) Å V = 3799.3(2) $Å^3$
	as prepared ($1.5H_2O$)	after dehydration	after rehydration
2	a = 15.2819(3) Å c = 19.7597(5) Å V = 3996.4(2) $Å^3$	a = 15.2738(4) Å c = 19.7526(5) Å V = 3990.7(2) $Å^3$	a = 15.2785(4) Å c = 19.7620(5) Å V = 3995.1(2) $Å^3$

X-Ray Crystallographic Analyses. Single crystals for X-ray structural analyses were separated manually from the reaction mixtures. The crystal structures were solved by direct methods and were refined by full-matrix least-squares techniques with the use of the SHELX package.[12] The structure was first refined without water molecules, leading to significant remaining electronic density peaks (ρ_{min} = −2.8 $e^-/Å^3$ and ρ_{max} = +5.2 $e^-/Å^3$ for **1** and ρ_{min} = −1.8 $e^-/Å^3$ and ρ_{max} = +5.9 $e^-/Å^3$ for **2**) and to the following final R values: R_1 = 0.057 and wR_2 = 0.17 for **1** and R_1 = 0.06 and wR_2 = 0.20 for **2**. Attempts to refine these peaks as oxygen from water molecules did not lead to realistic models even when using partial occupations or constraints on atomic displacement parameters. This feature indicates that water is strongly delocalized within the channels. Then, the SQUEEZE function of the PLATON software package[13] was used in order to remove the electron density in the channel of **1**. Afterward, cycles of refinements were carried out until convergence was reached, leading to (*i*) improvement of the R values and (*ii*) a significant decrease of remaining positive electronic density peaks as well as a smaller discrepancy between the absolute values of ρ_{min} and ρ_{max} (ρ_{min} = −2.9 and ρ_{max} = +2.5 for **1** and ρ_{min} = −2.6 and ρ_{max} = +3.9 for **2**). All non-hydrogen atoms were refined anisotropically. The positions of hydrogen atoms of pyrazine ligands correspond to their geometrical positions, and they were refined using the riding model. Crystallographic data as well as details of data collection and refinement for complexes **1** and **2** are given in Table 2. The unit cell contains one crystallographically independent cluster unit. The S3 and Br1 (μ_3 ligands) atoms lie in the 4d position (1/3, 2/3, z) on the 3-fold axis that permeates through the center of the molecule. Three terminal Br ligands are coordinated to the three Re's of the cluster face-capped by the μ_3-Br ligand. The three other Re atoms are coordinated to pyrazine, leading to the formation of the fac isomer. The representation of *fac*-$Re_6Q^i_7Br^i(pyz)^a_3Br^a_3$ in **1** is shown in Figure 1.

(10) Thomson, P.; Cox, D. E.; Hastings, J. B. *J. Appl. Crystallogr.* **1987**, *20*, 79.
(11) Petricek, V.; Dusek, M. *The Crystallographic Computing System JANA2000*; Institute of Physics: Praha, Czech Republic, 2000.
(12) Sheldrick, G. M. *SHELXTL DOS/Windows/NT*, version 5.10; Bruker Analytical X-Ray: Madison, WI.
(13) (a) Spek, A. L. *Acta Crystallogr.* **1990**, *A46*, C34. (b) Spek, A. L. *PLATON*; Utrecht University: Utrecht, The Netherlands, 2000.

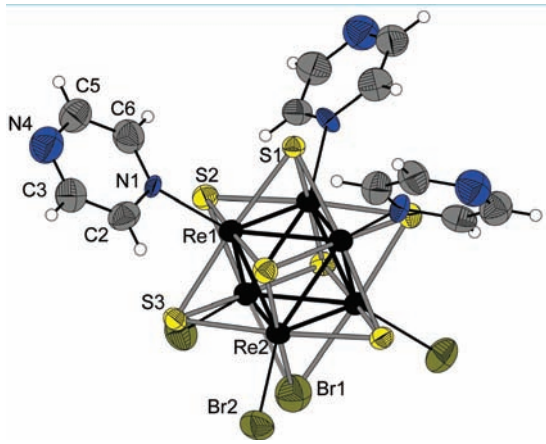

Figure 1. *fac*-$Re_6S^i_7Br^i(pyz)^a_3Br^a_3$ unit in **1**.

Table 2. Crystallographic Data of **1** and **2** from Single-Crystal X-Ray Diffraction Investigations

	1	**2**
empirical formula	$C_{12}H_{12}Br_4N_6Re_6S_7$	$C_{12}H_{12}Br_4N_6Re_6Se_7$
fw	1901.54	2229.84
cryst syst	trigonal	trigonal
space group	$P\bar{3}c1$	$P\bar{3}c1$
a (Å)	15.1186(3)	15.2693(5)
c (Å)	19.3798(7)	19.7243(8)
V (Å^3)	3836.2(2)	3982.6(2)
Z	4	4
ρ_{calc} (g/cm^3)	3.295	3.716
μ (mm^{-1})	23.418	28.587
cryst size (mm)	0.07 × 0.05 × 0.02	0.06 × 0.06 × 0.03
T_{min}; T_{max}	0.636; 0.258	0.451; 0.201
θ range, (deg.)	1.56−26.37	1.54−25.82
number of collected reflns	23124	26307
unique reflns	2605	2558
R_{int}	0.0617	0.0838
number of refined params	94	94
$R_1(F)$ [$F_o^2 > 2\sigma(F_o^2)$]	0.0534	0.0557
$R_w(F^2)$ (all data)	0.1628	0.1690

Results and Discussion

Synthesis and Structure. Holm et al., Zheng et al., and Sasaki et al. have developed, for a long time, the coordination chemistry of octahedral rhenium clusters. This chemistry is based on the replacement in solution of halogen apical ligands by functional organic donor ligands (e.g., pyridine or phosphine derivative) starting from the $[(n\text{-}C_4H_9)_4N]_3[Re_6Se^i_8X^a_6]$ precursor (X = halogen). In the literature, many examples of octahedral rhenium clusters functionalized by organic ligands are reported.[3−14] However, only two examples of rhenium cluster complexes coordinated to pyrazine, $[(n\text{-}C_4H_9)_4N]_2[trans\text{-}Re_6S^i_8(pyz)^a_2Cl^a_4]$ and $[(n\text{-}C_4H_9)_4N]_2[cis\text{-}Re_6S^i_8(pyz)^a_2Cl^a_4]$, are known.[15] They were prepared by the direct reaction in solution of $[(n\text{-}C_4H_9)_4N]_3[Re_6S^i_8Cl^a_6]$ and pyrazine. On the other hand, few examples of fac isomers of octahedral rhenium clusters were reported. $[(n\text{-}C_4H_9)_4N][fac\text{-}Re_6Se^i_8(PEt_3)^a_3I^a_3]$ was obtained in small yield by the reaction of $[(n\text{-}C_4H_9)_4N]_3[Re_6Se^i_8I^a_6]$ with an excess of PEt_3 in CH_3CN.[4b] After removal of the apical ligands using silver salts, the *fac*-$[Re_6Se^i_8(PPh_3)^a_3(CH_3CN)^a_3](SbF_6)_2$ and *fac*-$[Re_6Se^i_8(PPh_3)^a_3(isonicotinamide)^a_3](SbF_6)_2$ derivatives were obtained.[3b] Recently, a new technique has been developed for the functionalization of the Re_6 cluster. It simply consists of the reaction of an inorganic Re_6 cluster precursor with a molten organic functional ligand. The reaction between $Cs_3Re_6Q_7Br_7\cdot H_2O$ and molten EPh_3[7] results in the formation of *fac*-$[Re_6Q^i_7Br^i(EPh_3)^a_3Br^a_3]$ (Q = S, Se; E = P, As, Sb) in high yield. Note that *cis*-$[Re_6S^i_6Br^i_2(PPh_3)^a_2Br^a_4]$ and *trans*-$[Re_6S^i_6Br^i_2(PPh_3)^a_2Br^a_4]$[7c] were obtained using $Cs_2Re_6S^i_6Br^i_2Br^a_6$ as a cluster precursor, whereas *cis*-$Re_6S^i_8(PPh_3)^a_4Br^a_2$[7c] and $Re_6S^i_8(pyz)^a_4Br^a_2$ (unpublished results) were obtained from $Cs_4Re_6S^i_8Br^a_6$. The melt organic route, compared to usual solution chemistry, exhibits at least two advantages: it works for both sulfur and selenium series, and it enables an easier crystallization of neutral functional units. Let us recall that the $Re_6S^i_8$ series were reported to be less reactive than their $Re_6Se^i_8$ homologs in solution chemistry. It turns out that the number of substituted apical ligands depends on the charge of the unit in the starting precursor. The easy formation of the stable CsBr inorganic salt in the organic melt must be the key point of this reaction.

Description of the Unit. First of all, it must be pointed out that, despite its bidentate nature, each pyrazine is bonded to only one Re_6 cluster. The Re−Re, Re−Q^i, Re−Br^i, Re−Br^a, and Re−N distances are tabulated in Table 2. The $Re_6Q^i_7Br^i$ cluster core in **1** and **2** is built up from a Re_6 cluster lying in a cube of ligands formed by seven Q's (Q = S, Se) and one Br. It is worth noting that, in the starting $Cs_3Re_6Q^i_7Br^iBr_6\cdot H_2O$ precursor, the seven Q's and Br are randomly distributed on the eight inner positions of the unit. The presence of only one Br atom among the inner ligands generates the local $C3_v$ symmetry for the $Re_6Q^i_7Br^iBr_6$ unit and does not enable the formation of isomers. Thus, owing to the orientational disorder, the average apparent symmetry of the $Re_6Q^i_7Br^iBr_6$ unit deduced from X-ray single crystal diffraction analysis is close to O_h in the starting precursor.

Surprisingly, in the structure of **1**, the $Re_6Q^i_7Br^i(pyz)^a_3Br^a_3$ unit is not submitted to orientationnal disorder, and the local C_{3v} of the unit symmetry is preserved. Such an ordering is not so usual in cluster chemistry since many structures based on cluster units with mixed ligands—that differ in charge or in size—are based on the orientational disorder of isomeric units.[16] The result is a higher apparent symmetry than the local one. Halogen/chalcogen ordering has however already been evidenced in $Cs_2Re_6S^i_6Br^i_2Br^a_6$, $Cs_3Mo_6I^i_6I^i_{2-x}Se^i_xI^a_6$, $[(PhCH_2)_3N]_3Mo_6Cl^i_7O^iCl^a_6$, *cis*-$Re_6Te^i_6Cl^i_2(TeCl_2)^a_2Cl^a_4$, $[(n\text{-}C_4H_9)_4N]_4[(Re_6S^i_5Cl^i_2O^iCl^{a-a}_5)_2O^{a-a}_{1/2}]$, *cis*- and *trans*-$Re_6Q^i_6Br^i_2(PPh_3)^a_2Br^a_4$, and *fac*-$Re_6Q^i_7Br^i(EPh_3)^a_3Br^a_3$ series as well as oxygen/sulfur ordering in $[(n\text{-}C_4H_9)_4N]_2$-

(14) (a) Chen, Z. N.; Yoshimura, T.; Abe, M.; Sasaki, Y.; Ishizaka, S.; Kim, H. B.; Kitamura, N. *Angew. Chem., Int. Ed.* **2001**, *40*, 239. (b) Chen, Z. N.; Yoshimura, T.; Abe, M.; Tsuge, K.; Sasaki, Y.; Ishizaka, S.; Kim, H. B.; Kitamura, N. *Chem.—Eur. J.* **2001**, *7*, 4447. (c) Yoshimura, T.; Umakoshi, K.; Sasaki, Y.; Sykes, A. G. *Inorg. Chem.* **1999**, *38*, 5557. (e) Zheng, Z.; Gray, T. G.; Holm, R. H. *Inorg. Chem.* **1999**, *38*, 4888.

(15) Yoshimura, T.; Umokoshi, K.; Sasaki, Y.; Ishizaka, S.; Kim, H.-B.; Kitamura, N. *Inorg. Chem.* **2000**, *39*, 1765.

(16) (a) Cordier, S.; Naumov, N.; Salloum, D.; Paul, F.; Perrin, C. *Inorg. Chem.* **2004**, *43*, 219. (b) Cordier, S.; Perrin, C. *J. Solid State Chem.* **2004**, *177*, 1017. (c) Naumov, N.; Cordier, S.; Perrin, C. *Solid State Sci.* **2005**, *7*, 1517. (d) Naumov, N.; Cordier, S.; Perrin, C. *Chem. Comm.* **2004**, 1126. (e) Kirakci, K.; Cordier, S.; Perrin, C. *Chem.—Eur. J.* **2006**, *12*, 6419.

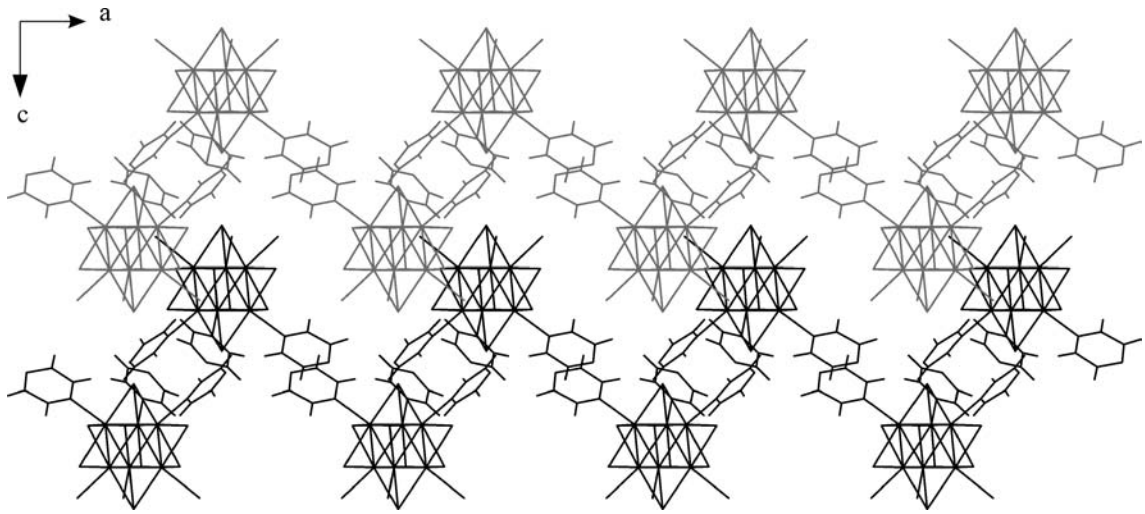

Figure 2. Representation of the stacking of two successive layers of units in *fac*-$Re_6S^i_7Br^i(pyz)^a_3Br^a_6 \cdot xH_2O$.

$[Re_6S^i_5Cl^i_2O^iCl^a_6]_2$ and $[Re_6S^i_6O^i_2(PPr_3)^a_6][Re_6S^i_6Cl^i_2Cl^a_6]\cdot CH_3CN$.[7,17] The ordering of μ_3-Br atoms in the hybrid structures **1** and **2** is the result of the selective substitution of three apical bromines by three pyrazine groups. One of the explanations of this selective ligand coordination is the specific distribution of electron density on the rhenium atoms in the starting precursor. Indeed, owing to the metal-to-ligand charge transfers, charge balances, and the stronger $Re-Q^i$ bond compared to the $Re-Br^i$ ones, the three rhenium atoms bonded to four μ_3-chalcogen ligands have a more positive charge than the three rhenium atoms bonded to three μ_3-chalcogen and one μ_3-halogen atom. The result is that the three $Re-Br^a$ bonds for which Re atoms are exclusively bonded to inner sulfur are weaker than the three opposite $Re-Br^a$ ones favoring the coordination of the neutral pyrazine nucleophilic ligands. This affords the fac isomer of a neutral trisubstituted hybrid unit with an ambivalent inorganic/organic character. The self-assembly of the latter building blocks leads to the formation of a unique structure in which the blocks are held together by halogen/chalcogen van der Waals contacts found in pure inorganic solids along with $\pi-\pi$ stacking and hydrogen bonds found in organic solids.

Each cluster interacts with three adjacent ones through $\pi-\pi$ stacking interactions as well as C−H···N bonds between pyrazine rings, building a zigzag hexagonal layer of clusters (Figure 2). The C−H···N bonds are in agreement with those reported in ref 18. The average distance between pyrazine rings is 3.6 Å for **1** and 3.7 Å for **2**. In the structure, the wavy layers are parallel to the *ab* plane, and they fit together according to an AA′A sequence (Figure 2). Considering one particular unit, the cohesion of the structure is due to (*i*) van der Waals contacts between μ_3-S3 and μ_3-Br1 along the *c* axis; (*ii*) van der Waals contacts between μ_3-S and μ_3-S and between μ_3-Br and μ_3-Br of three adjacent cluster units lying in the same plane but belonging to two successive layers; and (*iii*) N−H···N, C−H···Br^a, and C−H···Br^i bonds (Supporting Information). Note that the inner sulfur atoms are not involved in C−H···S^i nor N−H···S^i bonds, whereas all bromine ligands are involved in hydrogen bonds. Indeed, the formation of a robust hydrogen network involving μ-Br^i must be a driving force that contributes to the S/Br ordering. This important feature explains why a similar selenium/bromine ordering can occur in **2** despite similar ionic radii. The distances reported in Table 3 are in agreement with those tabulated in ref 19.

Table 3. Selected Bond Lengths (Å) for **1** and **2** from Single-Crystal X-Ray Diffraction

	1	**2**
	Intraunit Distances	
Re−Re	2.5836(8)−2.596(1)	2.6153(7)−2.628(1)
$Re-Q^i$	2.396(4)−2.455(4)	2.498(1)−2.531(2)
$Re-Br^i$	2.533(2)	2.580(2)
Re−N	2.267(7)	2.259(6)
$Re-Br^a$	2.525(4)	2.549(2)
	Interunit Distances	
$Br^i\cdots Q^i$	3.647(8)	3.618(3)
$Q^i\cdots Q^i$	3.491(8)	3.431(2)
$Q^i\cdots Br^a$	3.865(6)	3.774(3)
C−H···N	3.37(2)	3.419(9)
H···N	2.46(2)	2.520(7)
C−H···Br^i	3.766(7)	3.903(7)
H···Br^i	2.875(3)	3.009(1)
C−H···Br^a	3.623(9)	3.685(8)
H···Br^a	2.796(2)	2.858(1)

Description of the Channel. The AA′A packing of layers generates large tubular channels parallel to the *c* axis that are arranged according to a honeycomb disposition imposed by the trigonal symmetry of the *fac*-$Re_6Q^i_7Br^i(pyz)^a_3Br^a_3$ cluster unit. The minimal distances between the axis of the channel and the closest atoms has been found for hydrogen

(17) (a) Pilet, G.; Cordier, S.; Perrin, C.; Perrin, A. *J. Struct. Chem.* **2007**, *48*, 680. (b) Kirakci, K.; Cordier, S.; Perrin, C. *C. R. Chim.* **2005**, *8*, 1712. (c) Kirakci, K.; Cordier, S.; Shames, A.; Fontaine, B.; Hernandez, O.; Furet, E.; Halet, J.-F.; Gautier, R.; Perrin, C. *Chem.—Eur. J.* **2007**, *13*, 9608. (d) Mironov, Y. V.; Pell, M. A.; Ibers, J. A. *Inorg. Chem.* **1996**, *35*, 2709. (e) Simon, F.; Boubekeur, K.; Gabriel, J. C. P.; Batail, P. *Chem. Comm.* **1998**, 845. (f) Kozhomuratova, Z. S.; Naumov, N. G.; Naumov, D. Y.; Uskov, E. M.; Fedorov, V. E. *Russ. J. Coord. Chem.* **2007**, *33*, 213. (g) Uriel, S.; Boubekeur, K.; Batail, P.; Orduna, J.; Canadell, E. *Inorg. Chem.* **1995**, *34*, 5307. (h) Decker, A.; Simon, F.; Boubekeur, K.; Batail, P. *Z. Anorg. Allg. Chem.* **2000**, *626*, 309.
(18) Wardell, S. M. S. V.; Souza, M. V. N.; Wardell, J. L.; Low, J. N.; Glidewell, C. *Acta Crystallogr.* **2006**, *E62*, o3765.
(19) Rowland, R. S.; Taylor, R. *J. Phys. Chem.* **1996**, *100*, 7384.

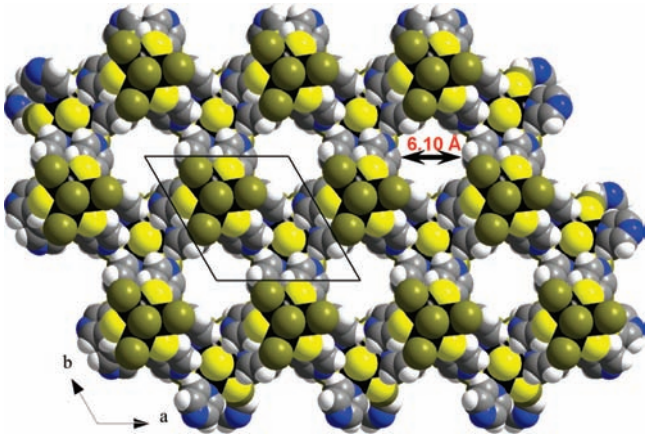

Figure 3. Projection of the structure of **1** along the *c* direction.

atoms (center-H = 4.153 Å for **1** and 4.315 Å for **2**). Taking into account a radius of 1.10 Å for H,[19] it means an effective aperture of about 6.10 Å for **1** and 6.43 Å for **2** (Figure 3). The axis of the channels merges with the $\bar{3}$-fold axes (0, 0, *z*) of the unit cell. The inner walls of the channels are mainly made from Q^i, Br^a, and H. The total free volume of the unit cell was found to be 43%, whereas the free volume available for solvent molecules calculated through the Platon procedures[13] is 29%. According to the wall constitution and to the size of the channels, H_2O molecules can easily be adsorbed through C−H···O, O−H···Q^i, or O−H···Br^a bonds. They have no effect in the stabilization of the structure and can be removed without collapsing the structures.

Comparison of the Structures of 1 and 2 with Those of Related Solid State Inorganic and Hybrid Organic/Inorganic M_6 Cluster Compounds. The hybrids **1** and **2** exhibit structural similarities with some solid-state cluster compounds. Indeed, many inorganic cluster solids crystallize in the trigonal system based on the stacking of compact hexagonal unit layers such as, for instance, the $Cs_2M_6X_{14}$[20] and $A_3M_6Q^i_{8-y}X^i_yX^a_6$ series (A = Rb, Cs; M = Mo, Re; X = I, Br; Q = S, Se).[17b,c] The trigonal symmetry of the octahedral M_6 cluster favors the formation of compact hexagonal layers, and their stacking enables the formation of channels with a honeycomb arrangement within the unit cell. The simplest structure is that of $Cs_2M_6X_{14}$ for which the hexagonal compact layers are stacked according to an ABA sequence. One half of the Cs^+ occupies voids between layers in the channels. The second half of the cesium cations lays within channels on specific Wyckoff positions. In this $Cs_2M_6X_{14}$ structure, the framework is stabilized by Coulombic interactions between cations and anionic cluster units. The $Cs_3Mo_6Br^i_7O^iBr^a_6$[17b] and $Cs_3Mo_6I^i_{8-x}Se^i_xI^a_6$[17c] series are based on noncompact unit layers stacked according to an ABC sequence that prevents the formation of channels. The van der Waals contacts between μ_3-chalcogens and μ_3-halogens occur between units that are stacked along 3-fold axes in a similar way to that found in **1** and **2**. In such ionic compounds that are stabilized exclusively by Coulombic interactions, intercalation or deintercalation properties are not expected. On the other hand, the $K_xKMo_{12}S_{14}$ ($0 \le x \le 1.6$) sulfide exhibits a tubular structure with a honeycomb disposition.[21] It is based on $Mo_{12}S^i_{14}S^a_6$ units resulting from monoaxial face-sharing condensation of the Mo_6S_{14} units. The units are organized in the same manner as that found in $Cs_2M_6X_{14}$ but with double S^{i-a}/S^{a-i} bridges between units to build a $[Mo_{12}S^i_8S^{i-a}{}_{6/2}]S^{a-i}{}_{6/2}$ framework. Indeed, the *x* K located in the channels can be removed and reintercalated or replaced by other cations (Li^+, NH_4^+). In the $KMo_{12}S_{14}$ framework, the minimum S···S interatomic distance is 6.71 Å, corresponding to a channel aperture roughly equal to 3.4 Å. The total accessible void for solvent represents 8.2% of the unit cell according to the Platon procedure. This very nice example of an inorganic tubular compound showed that the channel diameter in inorganic cluster materials formed by solid-state chemistry techniques is limited by the size of the inorganic ligands.

The association of large organic linkers directly grafted on octahedral clusters in the apical position should be an original strategy in order to obtain inorganic tubular cluster-based materials with larger channel diameters than those found in inorganic compounds. This can be achieved via solution chemistry (classical coordination chemistry below 100 °C or solvothermal synthesis between 100 and 250 °C[22]) or using organic melts, as reported in this work. If some hydrogen-bonded networks based on functionalized metal atom clusters have been reported in the literature,[3b,23a,b] at the present time, no open hybrid framework based on such functionalized units has been synthesized. Let us note that, some years ago, Batail and co-workers reported two organic/inorganic compact hybrids.[23b,c] They are based on Re_6 clusters in which the cluster core 3-fold symmetry is imposed via noncovalent bonding between clusters and organic moieties: $(TTF^{\bullet+})_3(Y^-)(Mo_6X^i_8X^a_6{}^{2-})$[23c] ($TTF^{\bullet+}$ = tetrathiafulvalene cation radical, Y = halogen) and $(EDT\text{-}TTF\text{-}CONH_2)_6[Re_6Se^i_8(CN)^a_6]$[23d] (EDT-TTF = ethylenedithiotetrathiafulvalene) with a molecular antiperovskite structure and a molecular Kagome hybrid network, respectively.

Comparison of the Structures of 1 and 2 with Those of Related Organic/Inorganic Hybrid Compounds Containing a Tubular Network. Looking to hybrids or organic compounds containing a tubular framework with a honeycomb disposition reported in the literature, one can consider three classes of compounds depending on the type of interaction between the inorganic building block and the organic counterpart. The first class is based on inorganic building blocks that are linked together by multidentate ligands sharing common donor atoms to form an extended 3D framework. The geometry of the inorganic building block and that of the organic linker are the key factors that govern the final topology of the framework. The most fascinating

(20) Kirakci, K.; Cordier, S.; Perrin, C. *Z. Anorg. Allg. Chem.* **2005**, *631*, 411.
(21) Picard, S.; Gougeon, P.; Potel, M. *Inorg. Chem.* **2006**, *45*, 1611.
(22) Férey, G. *Chem. Soc. Rev.* **2008**, *37*, 191.
(23) (a) Prokopuk, N.; Weinert, C. S.; Siska, D. P.; Ster, C. L.; Shriver, D. F. *Angew. Chem.* **2000**, *39*, 3312. (b) Oertel, C. M.; Sweeder, R. D.; Patel, S.; Downie, C. M.; DiSalvo, F. J. *Inorg. Chem.* **2005**, *44*, 2287. (c) Batail, P.; Livage, C.; Parkin, S. S. P.; Coulon, C.; Martin, J. D.; Canadell, E. *Angew. Chem.* **1991**, *30*, 1498. (d) Baudron, S. A.; Batail, P.; Coulon, C.; Clérac, R.; Canadell, E.; Laukhin, V.; Melzi, R.; Wzietek, V.; Jérome, D.; Auban-Senzier, P.; Ravy, S. *J. Am. Chem. Soc.* **2005**, *127*, 11785.

MOF with a hexagonal architecture is undoubtedly the MIL 88 series discovered by Férey's group.[24] This series of hybrids is based on the connection of chromium (or iron) trimers that share μ_3-O with symmetric dicarboxylate groups, leading to the formation of tunnels along the *c* axis arranged according to a honeycomb disposition along with bipyramidal cavities. This unusual framework is very flexible and enables very large volume variations when it interacts with solvent molecules. Other interesting related extended open MOFs are ZnF(AmTAZ) and the related ZnF(Am_2TAZ) and ZnF(TAZ) (TAZ = 1,2,4 triazole, AmTAZ = 3-amino-1,2,4 triazole, Am_2TAZ = 3,5-diamino-1,2,4 triazole).[25] Their structures consist of a 3D tubular framework that can be depicted as the association of ZnF_2N_3 moieties and 1,2,4 triazole groups by common nitrogen atoms. Layers of hexametallomacrocycles are made from six Zn^{2+} and six Am_2TAZ's held together through Zn−N bonds. Honeycomb tubular channels are generated by the connection of layers through common μ_2-F ligands and Zn−N interactions. The channel diameter is 4.7 Å, but it reaches 6.3 Å by replacing Am by hydrogen.

The second class consists of compounds whose structure is based on 2D layers built up from both hydrogen bonds and sharing ligands, as illustrated by the example of $[\{Cu_3(\mu_3\text{-}OH)(pz)_3(Cl)_2(Hpz)_3(H_2O)\}_2\{CuCl_2(Hpz)_2\}]$ (Hpz = pyrazole)[26] that crystallizes in the $R\bar{3}$ space group. The heptanuclear $[\{Cu_3(\mu_3\text{-}OH)(pz)_3(Cl)_2(Hpz)_3(H_2O)\}_2\{CuCl_2(Hpz)_2\}]$ complex is formed by the association of two $\{Cu_3(\mu_3\text{-}OH)(\mu_3\text{-}pz)_3(Cl)_2(Hpz)_3(H_2O)\}$ units weakly "bridged" by the copper atom of a $\{CuCl_2(Hpz)\}$ fragment. The organization of the MOF is due to supramolecular coordinative interactions involving one Cl and one Cu from two trinuclear units belonging to two nearby heptanuclear complexes. Each of these interactions is strengthened by a corresponding hydrogen bond involving the second Cl and the hydroxyl hydrogen from the trinuclear units. It results in a layer containing hexagonal holes with an architecture similar to that described for **1** and **2**. The holes of adjacent sheets match in such a way that parallel channels with a honeycomb disposition are generated through $\pi-\pi$ interaction of adjacent pyrazole groups. In this compound, the water is bonded to copper, and its desorption has not been evidenced. The effective free pore opening is 4.2 Å, and the total free cell volume represents 9% of the unit cell.

Finally, the third class to which **1** and **2** belong is that of PTMTC (perchlorotriphenylmethyl radical functionalized by three carboxylic groups).[27] The crystallization of these radicals that exhibit a trigonal symmetry, as found in the title building unit, leads to the formation of a 2D layer in which the PTMTC moieties are linked together via hydrogen bonds. The chlorine−chlorine contacts between neighboring layers enable the generation of hexagonal tubular channels with a diameter of 5.2 Å along with smaller pores with a diameter of 3 Å. This gives solvent-accessible voids of 15% of the total unit-cell volume. The location of carboxylic groups at inner walls of the hexagonal channels gives to these pores a highly polar and hydrophilic environment.

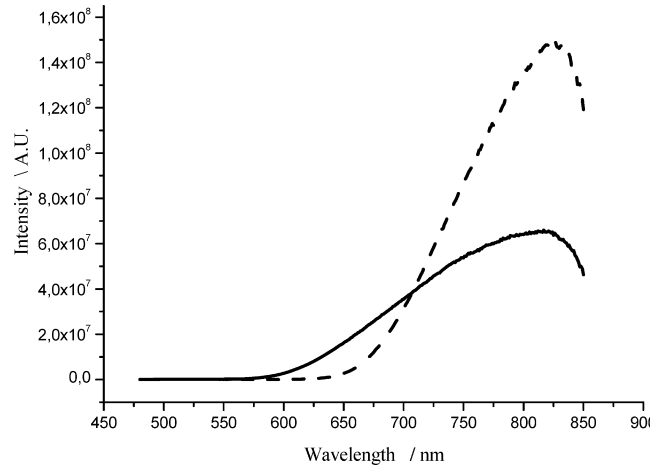

Figure 4. Luminescence spectra of **1** (bold line) and **2** (dashed line).

Luminescence Properties. The emission spectra of **1** and **2** are represented in Figure 4. Both compounds show a broad luminescence emission with maximums at about 821 nm for **1** and 824 nm for **2**. Usually the maximum of emission for the octahedral rhenium clusters with organic ligands varies in the range from 750 to 780 nm.[14] Complexes **1** and **2** constitute some of the few octahedral rhenium cluster complexes with low symmetry, which exhibit luminescence properties. Complex **1** is the first example of a complex in which the $Re_6S^i{}_7Br^i$ cluster core displays luminescence. In recent works, it was observed that the cluster compounds containing *fac*-$[Re_6S^i{}_7Br^i(EPh_3)^a{}_3Br^a{}_3]$ do not exhibit luminescence properties.[7c,d] Indeed, it is worth noting that the dispositions of ligands in **1** and *fac*-$[Re_6S^i{}_7Br^i(EPh_3)^a{}_3Br^a{}_3]$ are similar but the luminescence properties are different. Owing to the insolubility of **1** and **2**, at the present time, it is not possible to conclude whether the observed luminescence properties in **1** and the red shift are due to the coordination of pyrazine on the cluster, to the low symmetry of the unit, or to cooperative interactions between units within the solid. The luminescent spectra of dehydrated species are not significantly different from those reported here for **1** and **2**.

Concluding Remarks

In this work, we have synthesized under mild conditions and characterized the first members of luminescent MOFs

(24) (a) Surblé, S.; Serre, C.; Mellot-Draznieks, C.; Millange, F.; Férey, G. *Chem. Comm.* **2006**, 284. (b) Serre, C.; Surblé, S.; Mellot-Draznieks, C.; Audebrand, N.; Filinchuk, Y.; Férey, G. *Science* **2007**, *315*, 1828.

(25) (a) Su, C. Y.; Goforth, A. M.; Smith, M. D.; Pellechia, P. J.; Zur Loye, H. C. *J. Am. Chem. Soc.* **2004**, *126*, 3576. (b) Goforth, A. M.; Su, C. Y.; Hipp, R.; Macquart, R. B.; Smith, M. D. P. J.; Zur Loye, H. C. *J. Solid State Chem.* **2005**, *178*, 2511.

(26) Casarin, M.; Cingolani, A.; Di Nicola, C.; Falcomer, D.; Monari, M.; Pandolfo, L.; Pettinari, C. *Cryst. Grow. Des.* **2007**, *7*, 677.

(27) (a) Maspoch, D.; Domingo, N.; Ruiz-Molina, D.; Wurst, K.; Vaughan, G.; Tejada, J.; Rovira, C.; Veciana, J. *Angew. Chem., Int Ed.* **2004**, *43*, 1828. (b) Maspoch, D.; Ruiz-Molina, D.; Wurst, Domingo, N.; Cavallini, M.; Tejada, J.; Rovira, C.; Veciana, J. *Nat. Mater.* **2003**, *2*, 190.

having a porous architecture based on inorganic metal atom clusters associated with organic ligands. We showed that the trigonal geometry of octahedral clusters is favorable to the formation of honeycomb channels in solid-state compounds prepared at high temperatures, but their diameters are limited by the radii of inorganic ligands (halogen or chalcogen). The association of the Re_6 inorganic cluster with pyrazine reported here enables the formation of a hybrid compound containing a tubular framework with a honeycomb disposition. The channels have a larger aperture than those found in inorganic compounds, as for instance in $K_xKMo_{12}S_{14}$. However, despite the bidentate nature of pyrazine, **1** and **2** are not based on a 3D or 2D extended framework, as reported in many compounds with honeycomb channels. They are built up from neutral *fac*-$Re_6Q^i_7Br^i(pyz)^a_3Br^a_3$ compounds that are held together by supramolecular interactions in a similar way to that found in PTMTC. In **1** and **2**, owing to the size of the cluster building blocks, the total accessible amount of voids for solvent molecules is 29% versus 15% for PTMTC. The water molecules adsorbed within the channels can be removed without the collapsing of the structure. Further studies are now planned in order to learn more about the dynamic adsorption properties of these new promising materials.

Acknowledgment. This research is supported by PECO-NEI (No. 370) and ECO-NET (No. 18845 ZH) grants. Russian Foundation for Basic Research (Grants 08-03-90413 and 06-03-89503-HHC) and Fondation Langlois are acknowledged for financial support.

Supporting Information Available: Crystallographic data for **1** and **2**, TGA curves, detailed representation of interunit interactions, projection and view of structure, and the X-ray powder patterns for **2** (PDF). This material is available free of charge via the Internet at http://pubs.acs.org.

IC8018277